Bioorganic & Medicinal Chemistry 18 (2010) 3823–3833

Contents lists available at ScienceDirect

Bioorganic & Medicinal Chemistry

journal homepage: www.elsevier.com/locate/bmc

Simple di- and trivanillates exhibit cytostatic properties toward cancer cells resistant to pro-apoptotic stimuli

Delphine Lamoral-Theys [a], Laurent Pottier [b], Frédéric Kerff [e], François Dufrasne [c], Fabien Proutière [b], Nathalie Wauthoz [d], Philippe Neven [f], Laurent Ingrassia [b], Pierre Van Antwerpen [c], Florence Lefranc [b], Michel Gelbcke [c], Bernard Pirotte [f], Jean-Louis Kraus [g], Jean Nève [c], Alexander Kornienko [h], Robert Kiss [b,*], Jacques Dubois [a]

[a] Laboratoire de Chimie Analytique, Toxicologie et Chimie Physique Appliquée, Institut de Pharmacie, Université Libre de Bruxelles (ULB), Brussels, Belgium
[b] Laboratoire de Toxicologie, Institut de Pharmacie, Université Libre de Bruxelles (ULB), Brussels, Belgium
[c] Laboratoire de Chimie Pharmaceutique Organique, Institut de Pharmacie, Université Libre de Bruxelles (ULB), Brussels, Belgium
[d] Laboratoire de Pharmacie Galénique et Biopharmacie, Institut de Pharmacie, Université Libre de Bruxelles (ULB), Brussels, Belgium
[e] Centre d'Ingéniérie des Protéines, Institut de Chimie B6, Université de Liège, Liège, Belgium
[f] Laboratoire de Chimie Pharmaceutique, Centre Interfacultaire de Recherche du Médicament, Faculté de Médecine et de Pharmacie, Université de Liège, Liège, Belgium
[g] Laboratoire de Chimie Biomoléculaire, CNRS, IBDML-UMR-6216, Campus de Luminy Case 907 13288, Marseille cedex 09, France
[h] Department of Chemistry, New Mexico Institute of Mining and Technology, Socorro, NM 87801, USA

ARTICLE INFO

Article history:
Received 10 December 2009
Revised 8 April 2010
Accepted 16 April 2010
Available online 21 April 2010

Keywords:
Polyphenol
Kinase
Cancer
Apoptosis resistance
Cytostatic activity

ABSTRACT

A series of 33 novel divanillates and trivanillates were synthesized and found to possess promising cytostatic rather than cytotoxic properties. Several compounds under study decreased by >50% the activity of Aurora A, B, and C, and WEE1 kinase activity at concentrations <10% of their IC_{50} growth inhibitory ones, accounting, at least partly, for their cytostatic effects in cancer cells and to a lesser extent in normal cells. Compounds **6b** and **13c** represent interesting starting points for the development of cytostatic agents to combat cancers, which are naturally resistant to pro-apoptotic stimuli, including metastatic malignancies.

1. Introduction

Cancer remains a devastating disease and the number of cancer-related deaths is increasing. More than 90% of cancer patients die from tumor metastases.[1] Metastatic cancer cells are intrinsically resistant to apoptosis and, therefore, unresponsive to a large majority of anticancer drugs available today, because the latter generally work through apoptosis induction.[2–5] As a barrier to metastasis, cells normally undergo apoptosis after they lose contact with extracellular matrix or neighboring cells.[1] This cell death process has been termed 'anoikis'.[1] Tumor cells that acquire malignant potential have developed mechanisms to resist anoikis and thereby survive after detachment from their primary site when they travel through the lymphatic and circulatory systems.[1] Furthermore, many cancers are naturally resistant to apoptosis and, thus, associated with dismal prognoses. These include glioblastoma (GBM), the height of malignancy in the glioma group (the most common primary brain cancer),[6] melanomas,[7] esophageal cancers,[8] and non-small-cell-lung cancers (NSCLC),[9] among others. Thus, drug resistance, either acquired or intrinsic, is often related to inability of tumor cells to undergo apoptosis, resulting in cancer cell survival and treatment failure.[2,3] One solution to apoptosis resistance entails the complementation of cytotoxic therapeutic regimens with cytostatic agents, such as drugs targeting specific protein tyrosine kinases or membrane receptors.[4–6,10,11]

Natural polyphenols, including for example the green tea polyphenol (−)-epigallocatechin-3-gallate (EGCG),[12] genistein,[13] and curcumin,[14] are intensely investigated as potential anticancer agents, because they are able to inhibit multiple enzyme activities and signal transduction pathways, resulting in suppression of cell proliferation (e.g., inducing cytostatic effects) and enhancement of apoptosis (e.g., the cytostatic effects that end with cytotoxic

Abbreviations: ATCC, American type culture collection; DSMZ, Deutsche Sammlung von Mikroorganismen and Zellkulturen; ECACC, European collection of cell culture; GBM, glioblastoma; MTT, 3-(4,5)-dimethylthiazol-2-yl)-2,5-diphenyltetrazolium bromide; NSCLC, non-small-cell-lung carcinoma; QVM, quantitative videomicroscopy; RA, residual activity.

* Corresponding author. Tel.: +32 477 62 20 83; fax: +322 332 53 35.
E-mail address: rkiss@ulb.ac.be (R. Kiss).

0968-0896/$ - see front matter © 2010 Elsevier Ltd. All rights reserved.
doi:10.1016/j.bmc.2010.04.047

ones), as well as inhibition of cell invasion, angiogenesis, and metastases.[12–19]

In this paper we describe a novel series of di- and trivanillate-based polyphenols with cytostatic anticancer activity in vitro, as evidenced by computer-assisted phase-contrast microscopy (quantitative videomicroscopy).[20,21] We chose scaffolds incorporating two and three vanillic ester moieties because vanillin displays anticancer activity of its own, including anti-metastatic effects.[22,23] Some of the divanillates synthesized in the current work display structural similarities with curcumin, which therefore was used as an internal control.

Thirty-three compounds were synthesized and their IC_{50} in vitro growth inhibitory values were determined by means of the MTT colorimetric assay[20,21] in nine human and one mouse cancer cell lines. Because the MTT colorimetric assay can be problematic when reducing compounds such as polyphenols are assayed,[24] we also employed quantitative videomicroscopy[20,21] to validate the obtained data. The panel of 10 cancer cell lines under study included four cell lines for which we accumulated experimental evidence indicating that they display high levels of resistance to pro-apoptotic stimuli. These four cell lines include the human U373[20,25] and T98G[25] glioblastoma, the human A549 non-small-cell-lung carcinoma (NSCLC)[9,26] and the human OE21 esophageal cancer.[27] In contrast, we also obtained experimental evidence for the sensitivity to pro-apoptotic stimuli of human Hs683 oligodendroglioma,[25] human MCF-7 breast cancer,[28] human PC-3 prostate cancer[28] and mouse B16F10 melanoma[29] cell lines. Compound-induced modifications in cell morphology and cell proliferation were monitored by means of quantitative videomicroscopy.[20,21] Sixteen of the 33 compounds under study were further evaluated with MTT colorimetric assay and computer-assisted phase-contrast microscopy in two human normal (fibroblast) cell lines in order to determine their bioselectivity. The ability of most of the compounds under study to inhibit Aurora A, B, and C, and WEE1 kinase activity have then been determined after having characterized the effects of divanillate **6b** on a panel of 256 kinases in order to characterize its multi-kinase inhibitor profiles.

2. Results and discussion

2.1. Chemistry

Using the above-mentioned report on vanillin,[22,23] we opted to proceed with simple linear and branched diols and triols. To this end, esterification reactions of diversely substituted benzoic acids **1a**–**1d** with linear alkane diols and dibromides of varying chain length were investigated (Scheme 1). In the presence of the free phenol functionality in **1a**–**1d**, esterification using dicyclohexylcarbodiimide (DCC) and dimethylaminopyridine (DMAP) did not furnish the desired products regardless of the length of the alkyl chain. In contrast, alkylation reactions with dibromoalkanes allowed us to obtain directly in one step the desired diesters with $n \geqslant 4$ (**4a**, **4b**, **5b**, **6a**, **6b**, **6c**, **6d**, **7a**, **7b**, **7c**, **7d**, **8b**, **9b**, **9d**, **10b**, and **11b**) in 7–72% yields. In addition to compounds containing the vanillic moiety, we obtained analogues incorporating dimethoxybenzoic (**6a** and **7a**), isovanillic (**6c** and **7c**), and dihydroxybenzoic ester residues (**6d**, **7d**, and **9d**). Unfortunately, the corresponding alkylations with dibromoethane and dibromopropane ($n = 2$ and 3) only led to the formation of mono-esters, probably as a result of bromide hydrolysis by way of anchimeric assistance in medium-sized mono-ester intermediates. Therefore, the short-chain products **2b** and **3b** were synthesized using a three-step procedure starting from ethylene and propylene glycols and involving the protection of the phenolic function as benzyl ether (Scheme 2). Thus, vanillic acid was reacted with benzyl chloride to afford **1bBn** in 63% yield. Subsequent esterification with *n*-alkyl diols ($n = 2$ and 3) and hydrogenolysis then gave the desired divanillates **2b** and **3b** in 21% and 25% overall yields, respectively.

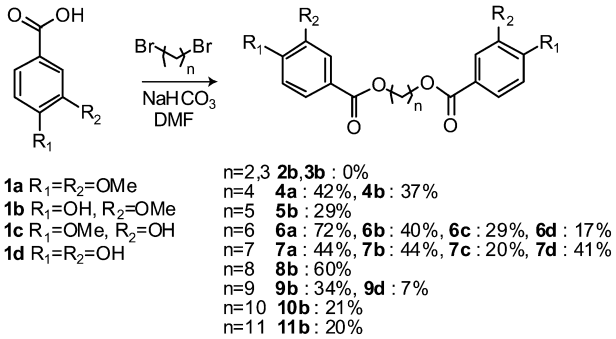

1a R_1=R_2=OMe
1b R_1=OH, R_2=OMe
1c R_1=OMe, R_2=OH
1d R_1=R_2=OH

n=2,3 **2b**,**3b** : 0%
n=4 **4a** : 42%, **4b** : 37%
n=5 **5b** : 29%
n=6 **6a** : 72%, **6b** : 40%, **6c** : 29%, **6d** : 17%
n=7 **7a** : 44%, **7b** : 44%, **7c** : 20%, **7d** : 41%
n=8 **8b** : 60%
n=9 **9b** : 34%, **9d** : 7%
n=10 **10b** : 21%
n=11 **11b** : 20%

Scheme 1.

Using various commercially available alkylating agents, we expanded the diversity of our polyphenols by preparing compounds incorporating unsaturated (**4f** and **4g**) and aromatic (**12a** and **12b**) linkers as well as trisubstituted analogues (**13a**–**13c**, Scheme 3). Because the alkylation yields decrease with the increase in the number of free phenol functions in the products (only 7% for tetraphenol **9d**), to obtain highly hydroxylated compounds, such as digallates **6e** and **7e**, we chose again the three-step route involving the protection of the phenolic functionality (Scheme 4). Compounds **6e** and **7e** were obtained in overall yields of 9% and 21%, respectively, by way of the benzylation, alkylation and deprotection sequence (Scheme 4).

Further, to increase the linker rigidity, we synthesized cyclohexanediol-based divanillates. Cyclohexane diols **14a**–**14c** and **15**, were esterified with the benzyl-protected vanillic acid (**1bBn**) and the benzyl group was removed by catalytic hydrogenation using palladium on charcoal to give **17a**–**17c** and **18** in 12–24% overall yields (Scheme 5). When the same procedure was applied to aminotriol **16** (chosen for the possibility of a positive charge at the core of the molecule), only the disubstituted analogue **19** was obtained in 3% overall yield over three steps.

Finally, as esters can be cleaved by esterases in biological media, we designed a more biologically stable, bioisosteric bis-tetrazole analogue **22a** (Scheme 6). A two-step procedure was envisaged: formation of the tetrazole **21** from the corresponding nitrile **20**[30] followed by alkylation under the same conditions used for benzoic acid derivatives. In the event, the major product was the less sterically hindered 2,5-2,5 regioisomer **22a**, but we also were able to isolate a small amount of the more hindered 1,5-2,5 regioisomer **22b** (Scheme 6). The structures of both regioisomers were confirmed by an NOE analysis (see the Supplementary data). The overall yields for **22a** and **22b** were 40% and 4%, respectively. The synthesis of bis-tetrazoles with free phenol functions is currently under investigation.

2.2. Pharmacological evaluation

2.2.1. Determination of the IC_{50} in vitro growth inhibitory values

Thirty-three compounds were synthesized in the current study and we utilized the MTT colorimetric assay to determine their IC_{50} in vitro growth inhibitory values in nine human and one mouse cancer cell lines. The histological origin of each cancer cell line is detailed in the legend to Table 1. As already mentioned in Section 1, we previously demonstrated high levels of resistance to pro-apoptotic stimuli for the human U373[20,25] and T98G[25] GBM, the A549 NSCLC,[9,26] and the OE21 esophageal cancer[27] cell lines. In the same manner, we demonstrated the sensitivity to apoptosis for the human

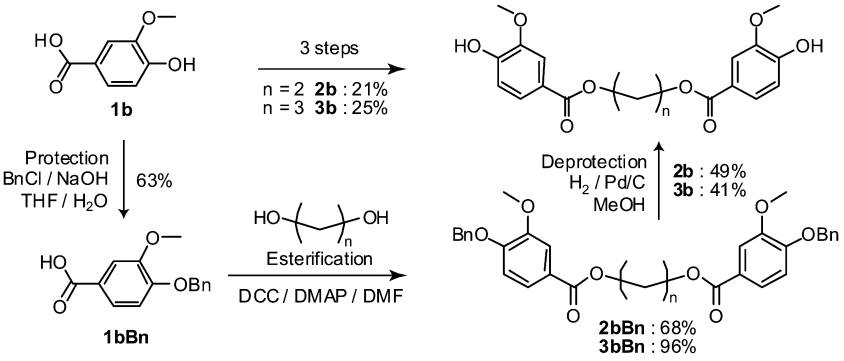

Scheme 2.

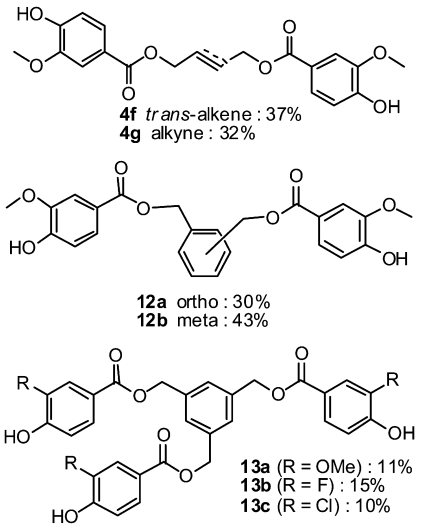

Scheme 3.

Hs683 oligodendroglioma,[25] MCF-7 breast cancer,[28] PC-3 prostate cancer,[28] and mouse B16F10 melanoma[29] cell lines. We observed no statistically significant (p >0.05) differences in the IC_{50} values for any compound under study between cancer cell lines that are sensitive or resistant to pro-apoptotic stimuli (Table 1). In the same manner, no differences in sensitivity were observed between the human and the mouse cancer cell lines (Table 1). This indicates that mouse cancer models can be used in the future to determine in vivo antitumor activity for the leads that will be derived from the presently investigated polyphenols.

We could not attain the 95% purity for 4 out of the 33 compounds under study, namely **8b**, **12a**, **18**, and **19** (Table 1). These compounds were withdrawn from further biological analyses. We used quantitative videomicroscopy (QVM) in order to potentially identify false positive compounds from the MTT assay data (Fig. 2).[24] All compounds that were characterized as active against a given cancer cell line (IC_{50} <100 μM) by means of the MTT colorimetric assay also appeared to be active against these cancer cells when assayed by means of QVM (data not shown). The same observation was made with respect to the inactive compounds (IC_{50} >100 μM). Thus, neither false positive nor false negative IC_{50} values exist in Table 1. However, while performing the QVM quality control experiments, we identified 6 of the 33 compounds, namely **4f**, **6a**, **6c**, **7a**, **22a**, and **22b**, which were not completely soluble in the biological media at their IC_{50} in vitro growth inhibitory concentration, as illustrated in Figure 2. We took this observation into account during the interpretation of the kinase assay-related data (vide infra).

The mean growth inhibitory IC_{50} values across the nine human cancer cell lines for the 24 out of 33 compounds for which the solubility and purity levels were reached are given in Figure 3. As is seen from these data, compounds **9b**, **10b**, and **11b** (divanillates incorporating two phenolic functions and the longest linker, $n \geqslant 9$), **7d** (divanillate incorporating four phenolic functions and an intermediate linker, $n = 7$), **13a**, **13c** (trivanillates) displayed the most potent in vitro antitumor activity. The IC_{50} in vitro growth inhibitory values obtained with these six compounds are on a par with those displayed by the most active natural polyphenols analyzed heretofore.[15] The anticancer activity did not seem significantly affected by the number of phenolic functions. Indeed, the potencies were similar (p >0.05) for the compounds incorporating 2 (**6b**, **7b**), 4 (**6d**, **7d**) or 6 (**6e**, **7e**) phenolic hydroxyls. In contrast, the C-chain length seemed to signif-

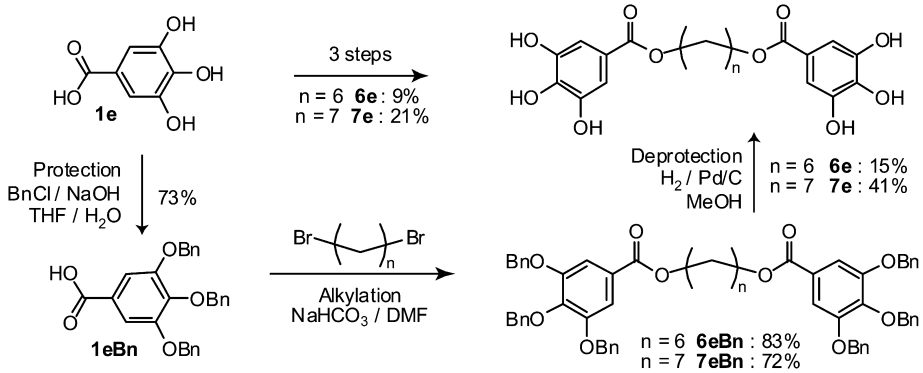

Scheme 4.

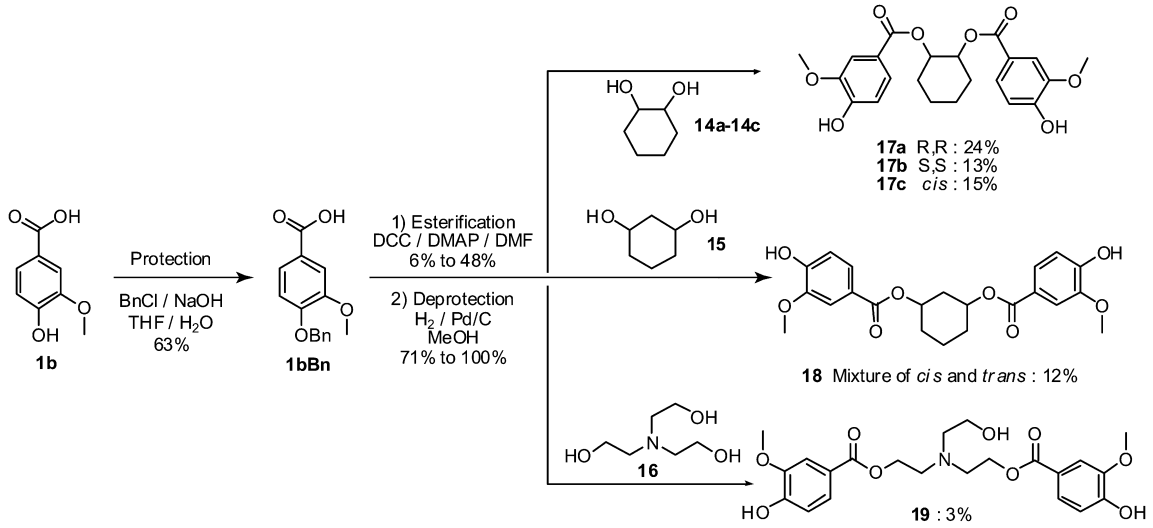

Scheme 5.

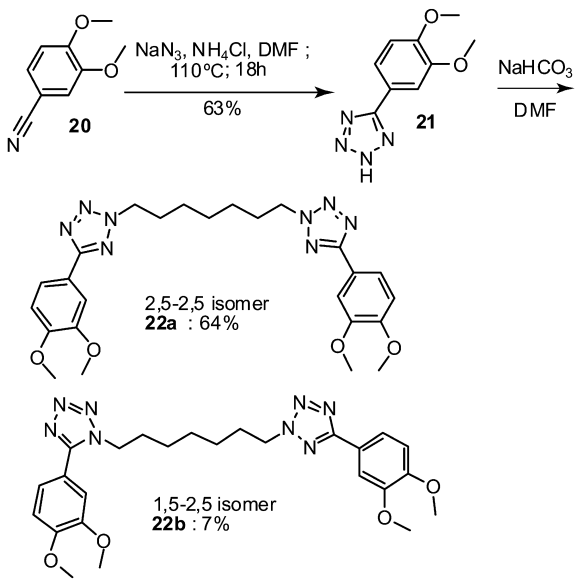

Scheme 6.

icantly influence in vitro anticancer activity with a progressive drop in potency with the increase in linker length from $n = 2$ to $n = 5$, and then the recovery of activity with longer linkers ($n = 6–11$). Finally, the replacement of the vanillic moiety (**6b**, **7b**) by the isovanillic one (**6c**, **7c**) brought about a partial loss of solubility for **6c** (Table 1). The replacement of the esters with bioisosteric tetrazoles (**22a**, **22b**) led to a loss of solubility (Table 1).

2.2.2. Compound bioselectivity

We define bioselectivity as the mean IC_{50} (normal cells lines)/mean IC_{50} (tumor cell lines) ratio. Table 2 reveals varied bioselectivity ratios for the compounds under study. First, increasing the length of the C-chain linker in divanillic polyphenols is paralleled by the drop in bioselectivity (Table 2), while the anticancer activity increases (Fig. 3). Second, adding the fluoro (**13b**) or chloro (**13c**) substituents to the trivanillate scaffold (**13a**) seems to increase bioselectivity (Table 2), with **13c** being significantly ($p < 0.01$) more active than **13b** in terms of in vitro anticancer activity (Table 1; Fig. 3). Figure 4 morphologically illustrates the levels of bioselectivity exhibited by **6b** and **13c**.

The data in Table 1 indicate that a number of our divanillates display growth inhibitory potencies similar to that of curcumin (**23**, Fig. 1), used as a reference for the divanillate-based polyphenols. However, Figure 4 reveals that curcumin displays cytotoxic effects at its IC_{50} in vitro growth inhibitory concentration, a feature that was not observed with compound **6b** (Fig. 4) sharing structural similarities with curcumin. These observations strongly suggest that curcumin exerts its antitumor effects through modes of action distinct from those associated with the divanillates under study, as also strongly suggested by the data we report below with respect to kinase activity measurements. Figure 4 also clearly shows that curcumin is considerably more toxic to normal Wi38 fibroblasts than **6b** or **13c**.

2.2.3. The compounds under study are cytostatic rather than cytotoxic

The QVM analyses clearly indicated that all compounds under study are cytostatic, not cytotoxic, as illustrated in Figure 4 for compounds **6b** and **13c**. The cells have not been washed and the medium together with the dead cells have not been removed before the pictures were taken. In fact, the quantitative videomicroscopy approach recorded all the events occurring on the bottom of the flask during a 72-h period of observation and less than 15% dead cells appeared during this period of observation, the reason why we claim that the compounds under study induce cytostatic rather than cytotoxic effects. In contrast, curcumin (**23**) clearly appears to be cytotoxic (Fig. 4), while displaying in vitro anticancer activity not higher than those displayed by the most active compounds under study (Fig. 3). Thus, the in vitro anticancer activity of our polyphenols is related to cell proliferation delay or blockade, rather than cell killing (Fig. 4). The sustained delay or blockade in cancer cell proliferation then in turn leads to cell death several days after the cells have been challenged with the compounds (data not shown). Flow cytometry analyses performed at random for various compounds under study revealed that none of them induced apoptosis during the three-day period that was used to determine the MTT colorimetric assay-related IC_{50} values of each compound (data not shown). The fact that compounds **6b** and **13c** induce cytostatic rather than cytotoxic anticancer effects prompted us to assay the inhibition activity of **6b** on a panel of 256 kinases.

Table 1
Determination of in vitro anticancer activity in nine human and one (B16F10) mouse cancer cell lines

Compounds	% Purity	% Stabil.[b]	# chem. synth. step[c]	In vitro IC_{50} growth inhibitory values[a] (μM; * = >100 μM; ** = >1000 μM)											QVM QC
				U373	T98G	HS683	LOVO	A549	MCF-7	PC-3	OE21	OE33	m ± SEM	B16F10	
1b	99	100	CA[d]	**	**	**	**	**	**	**	**	**	**	**	+
1bMe	99	100	CA	*	*	*	83	*	*	*	77	*	*	*	+
2b	100	100	3	41	59	82	10	69	45	57	56	63	54 ± 6	28	+
3b	98	96	3	*	*	*	50	*	89	88	*	64	>88	45	+
4b	96	100	1	98	91	*	54	65	80	67	*	67	>80	94	+
5b	99	99	1	69	*	*	94	*	*	*	*	*	>96	*	+
6b	96	100	1	22	56	63	34	27	39	39	68	63	46 ± 6	22	+
7b	96	96	1	44	58	50	44	51	56	44	46	47	49 ± 2	10	+
8b	89	100	1	38	45	40	94	39	35	30	62	28	46 ± 6	4	+
9b	96	100	1	36	32	27	24	24	27	36	28	28	29 ± 1	9	+
10b	96	98	1	30	30	25	28	30	23	26	28	28	28 ± 1	6	+
11b	95	98	1	31	32	22	29	21	25	25	27	28	27 ± 1	11	+
6c***[e]	98	100	1	68	*	50	30	54	55	90	44	52	>60	68	–
7c	96	97	1	35	31	30	18	32	25	42	34	36	31 ± 2	26	+
6a***	100	88	1	46	*	49	82	46	*	86	49	*	>73	*	–
7a***	100	100	1	*	*	46	41	43	44	43	53	64	>59	30	–
6d	95	100	1	54	24	44	44	46	69	88	49	55	53 ± 6	10	+
7d	100	96	1	31	11	10	26	18	21	44	41	34	26 ± 4	1	+
9d	95	97	1	37	31	24	34	32	28	68	37	45	37 ± 4	1	+
6e	96	100	3	52	45	53	48	72	53	81	31	73	56 ± 5	27	+
7e	96	98	3	35	38	32	43	30	58	44	43	66	43 ± 4	22	+
4f***	100	100	1	*	*	*	*	*	*	*	73	*	>97	57	–
4g	100	99	1	39	72	40	36	40	39	46	76	61	50 ± 6	36	+
12a***	84	99	1	65	64	47	46	48	44	42	56	66	53 ± 3	24	+
12b	96	97	1	66	46	58	26	63	57	42	34	45	49 ± 4	37	+
17a	99	97	3	20	70	57	44	43	47	59	41	66	50 ± 6	49	+
17b	98	96	3	53	*	*	64	76	75	77	45	77	>74	59	+
17c	100	97	3	43	76	49	28	38	46	35	55	56	47 ± 5	38	+
18***	90	95	3	27	72	69	31	65	32	34	46	55	48 ± 6	40	+
19***	82	97	3	*	*	95	78	*	80	87	81	*	>96	36	+
13a	100	97	1	28	28	27	29	23	55	30	16	19	28 ± 4	41	+
13b	98	98	1	37	37	25	48	26	41	44	73	71	44 ± 5	31	+
13c	97	98	1	31	25	31	33	26	33	36	28	40	31 ± 2	7	+
22a***	99	99	2	38	40	31	32	26	25	40	28	36	33 ± 2	38	–
22b***	96	96	2	91	55	80	41	52	71	*	81	*	>75	*	–
23	99	99	CA	18	25	22	24	27	24	33	27	35	26 ± 2	10	+

[a] The IC_{50} in vitro growth inhibitory concentrations were determined by means of the MTT colorimetric assay. The cell lines include the human U373 (ECACC code 89081403), T98G (ATCC code CRL1690), and Hs683 (ATCC code HTB-138) glioblastoma, the LoVo (DSMZ code ACC350) colon cancer, the A549 (DSMZ code ACC107) NSCLC, the MCF-7 (DSMZ code ACC115) breast cancer, the PC-3 (DSMZ code ACC465) prostate cancer, the OE21 (ECACC code 96062201), and OE33 (ECACC code 96070808) esophageal cancer.

[b] The stability of products was measured by HPLC analysis following incubation in a physiological solution at 37 °C over 7 days. Results are expressed as the percentage of the incubated compound recovered.

[c] Number of chemical synthetic steps to obtain the compound.

[d] CA: commercially available.

[e] The compounds labeled '***' have been withdrawn from kinase assay analyses because either not pure enough (purity <95%), not stable enough (stability at 37 °C for 7 days <85%) or precipitating at the IC_{50} concentration as revealed by quantitative videomicroscopy-related quality control (see the QVM QC column and Fig. 2).

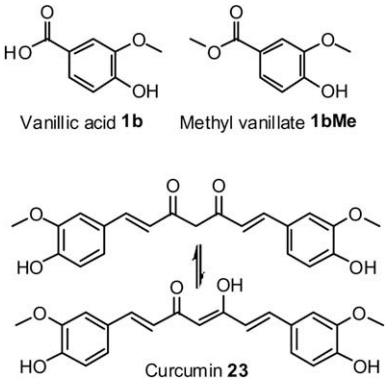

Figure 1. Structures of vanillic acid, methyl vanillate and curcumin.

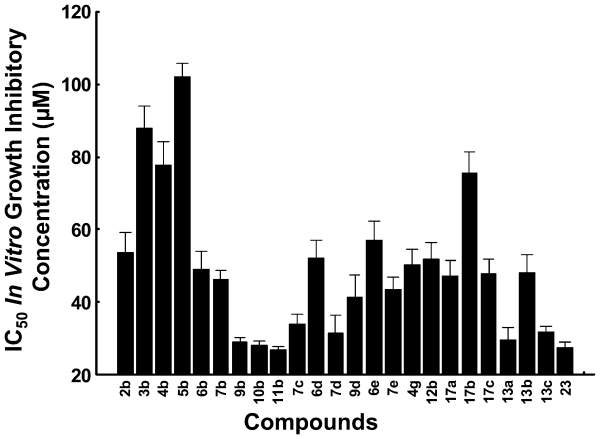

Figure 3. IC_{50} in vitro growth inhibitory concentrations for 25 out of 33 compounds for which the solubility and purity levels were reached, determined by means of the MTT colorimetric assay. The data are presented as means ± SEM calculated on nine values, each value representing in turn the mean value calculated on sextuplicates. The nine values correspond to the nine human cancer cell lines given in Table 1. When Table 1 reports a mean value >100 μM for a given cell line, we used the '105 μM' value in calculation of the mean ± SEM IC_{50} numbers. Thus, the loss of antitumor activity for the less active compounds is underestimated, while the potencies of the most active analogues are reflected accurately.

2.2.4. Divanillate 6b targets multiple kinases

Compound **6b**, which displays a bioselectivity index >2.2 (Table 2), was assayed at 20 μM on a panel of 256 human kinases. This 20 μM concentration represents ca. 50% of its IC_{50} in vitro growth inhibitory concentration (Table 1). At 20 μM **6b** decreased by >50% the activity of eight kinases, that is, Aurora A, Aurora B, Aurora C, CDK7/CycH, FER, SAK, WEE1, and WNK2 (data not shown). Aurora,[31,32] CDK7,[33,34] Fer,[35,36] SAK,[37,38] WEE1,[39] and WNK2,[40,41] that is, the kinases targeted by **6b**, are over expressed in various types of cancers and display major roles in cancer cell biology.

Cancer cells exhibit deregulation in multiple cellular signaling pathways and treatments using specific agents that target only one pathway usually fail in cancer therapy, especially for those cancer types that display natural resistance to pro-apoptotic stimuli.[32,42–48] As recently emphasized by Sarkar and Li,[49] combination treatments using chemotherapeutic agents with distinct molecular mechanisms are considered more promising and some natural products, including polyphenols, have growth inhibitory effects on human apoptosis-resistant cancer cells mediated by targeting multiple cellular signaling pathways without causing unwanted toxicity in normal cells. Well-known modes of action by which polyphenolic compounds exert their anticancer activity include for example redox-dependent and redox-independent mechanisms underlying cytotoxic/cytostatic effects toward tumor cells and cytoprotection of normal cells,[16] phototoxicity against tumor cells and photoprotection of non-tumor cells,[16] and inhibition of specific proteases[17] in addition to well-documented effects on cell cycle and/or the inhibition of the NF-κB pathway.[19] In contrast, the polyphenol-induced anticancer effects mediated through kinase targeting have not been studied adequately as we indicated in our recent review of this topic.[15] The polyphenol-related multikinase inhibition usually occurs in the double digit micromolar concentration range,[15] unlike that of synthetic small molecules designed to selectively inhibit the activity of a given kinase, which

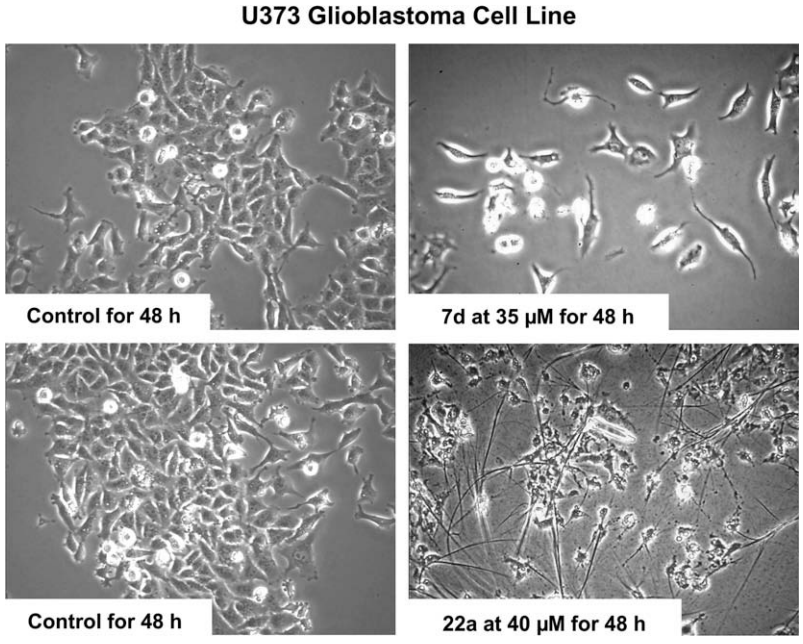

Figure 2. Quantitative videomicroscopy analyses of in vitro anticancer activity displayed by compounds **7d** and **22a** in the human U373 glioblastoma cell line. Compounds **7d** and **22a** were assayed at their IC_{50} in vitro growth inhibitory concentrations, that is, 32 and 35 μM, respectively (Table 1). Compound **22a** appeared non soluble in the biological media as illustrated by marked precipitation processes.

Table 2
Comparison of in vitro global cell population growth development in two human normal versus nine human cancer (see Table 1) cell lines

Compounds	In vitro IC_{50} growth inhibitory values (μM)				Ratio normal/cancer[b]
	Normal human cell lines			Human cancer cell line (mean[a])	
	WI38	NHDF	Mean		
2b	>100	92	>96	54	>1.8
3b	>100	>100	>100	>88	n.c.[c]
4b	>100	>100	>100	>80	n.c.
5b	>100	>100	>100	>96	n.c.
6b	>100	>100	>100	46	>2.2
7b	74	81	78	49	1.6
6d	86	72	79	53	1.5
7d	89	84	87	26	3.3
6e	>100	79	>90	56	>1.6
7e	>100	95	>98	43	>2.3
8b	61	89	75	46	1.6
9b	30	32	31	29	1.1
10b	46	29	38	28	1.3
13a	20	30	25	28	0.9
13b	74	69	72	44	1.6
13c	65	37	51	31	1.6

[a] The m ± SEM values were calculated from the values reported in Table 1.
[b] The mean IC_{50} value in the normal group was divided by the mean IC_{50} value in the cancer group. The normal cell lines analyzed include the human WI-38 (ATCC code CCL-75) and NHDF (Promo Cell c-12300) fibroblast cell lines.
[c] n.c. means 'not calculated'. The ratio was not calculated when both mean IC_{50} values in normal and cancer cell lines were associated with '>'.

often occurs in nanomolar concentrations.[31,44] The current data clearly show that several compounds under study (as detailed below) display multi-anti-kinase activity in single digit micromolar concentration range.

2.2.5. Characterization of anti-Aurora and anti-WEE1 kinase activity

Although not as potently as some of the specifically designed reported Aurora kinase inhibitors,[31,32] compound **6b** targeted the three Aurora kinases as detailed above. Figure 5A illustrates the dose–response inhibition curves for a dozen of compounds with respect to Aurora A kinase activity, including curcumin (**23**). We performed the same types of analyses with respect to Aurora B, Aurora C, and WEE1 kinases. However, we report in Figure 5B the μM concentrations inducing 50% decrease in Aurora A, B, C, and WEE1 kinases instead of illustrating each dose–response curve as in Figure 5A. We thus determined the IC_{50} inhibitory values of various divanillates (with curcumin as a reference) and trivanillates on the three Aurora kinases to compare with the WEE1 kinase that was also targeted by **6b** in our initial screening using a 20 μM concentration (data not shown). Incorporating 4 (**6d**, **7d**; data not shown) or 6 (**6e**, **7e**; Fig. 5B) phenolic hydroxyls leads to the ability of the compounds to progressively inhibit WEE1 activity in addition of inhibiting Aurora kinase activity. The same feature was observed when adding fluoro (**13b**) or chloro (**13c**) substituents on the trivanillate scaffold (**13a**) (Fig. 5B).

Curcumin (**23**), which shares structural similarities with divanillates such as **6b** and **7b**, displayed similar Aurora/WEE1 kinase inhibition profiles when compared to **6b** and **7b**, while exerting less potent activity inhibition than **6b** and **7b** (Fig. 5B). Curcumin did not inhibit WEE1 kinase activity, even at concentrations as high as 100 μM (Fig. 5B).

2.2.6. Molecular docking of 6b and 13c to Aurora A and Aurora B kinases

To further validate the role of Aurora kinase targeting in anticancer effects of our synthetic polyphenols, we performed molecular docking experiments. The best docking solution for compound **6b** on Aurora A is characterized by a binding energy of −7.2 kcal/mol. One of the vanillic esters binds in the purine binding pocket, allowing for favorable hydrophobic interactions and one hydrogen bond with the hinge region (Fig. 6A). The second vanillic ester binds in the hydrophobic pocket adjacent to the third phosphate-binding site, the ester being involved in two hydrogen bonds (Fig. 6A). The linker does not appear to make significant contributions. For compound **13c**, the lowest energy solution (−10.7 kcal/mol) gives a conformation very similar to compound **6b** with two phenols in almost identical positions (Fig. 6B). The third phenol covers Thr217, an active site residue not conserved in Aurora B and C. The third ester forms a hydrogen bond with a nitrogen backbone of the N-terminal lobe loop delimiting the upper side of the nucleotide-binding site.

The best solutions for these two compounds in Aurora B are different from the ones observed for Aurora A. In the lowest energy conformation of compound **6b** (−6.8 kcal/mol), the linker partially occupies the purine position and participates in hydrophobic interactions. In addition, one vanillic ester interacts with the hinge region, while the second one is in the sugar binding region making three hydrogen bonds, including one with Glu177 which substitutes Thr217 in Aurora B and C (Fig. 6C). On the other hand, in the best solution (−9 kcal/mol), compound **13c** virtually wraps around Glu177, with one ester group interacting with the hinge region, another one with the sugar region and the last one with the solvent accessible region (Fig. 6D).

According to AUTODOCK 4.1, the affinities of compound **6b** for Aurora A and B correspond to estimated inhibition constants (k_i) of about 5 μM. For **13c**, the estimated k_i are below 50 nM. The affinity of ATP for a kinase is usually considered to be around 10 μM. The binding energies reported are therefore compatible with a competitive inhibition of the Aurora kinases.

An additional factor that needs to be taken into account while analyzing the computer-generated solutions is flexibility of the kinase active site.[50,51]

2.2.7. Aurora kinase inhibition is responsible, at least partly, for the in vitro anticancer activity

We investigated whether the in vitro anticancer activity of the compounds under study could be related, at least partly, to Aurora kinase inhibition. We observed a weak but nevertheless statistically significant (p <0.05) correlation between the compound-induced inhibitory activities for the three Aurora kinases and their anticancer activities. Indeed, the compounds manifesting the highest anti-Aurora kinase activities, also display the highest in vitro anticancer activity. However, this analysis revealed the absence

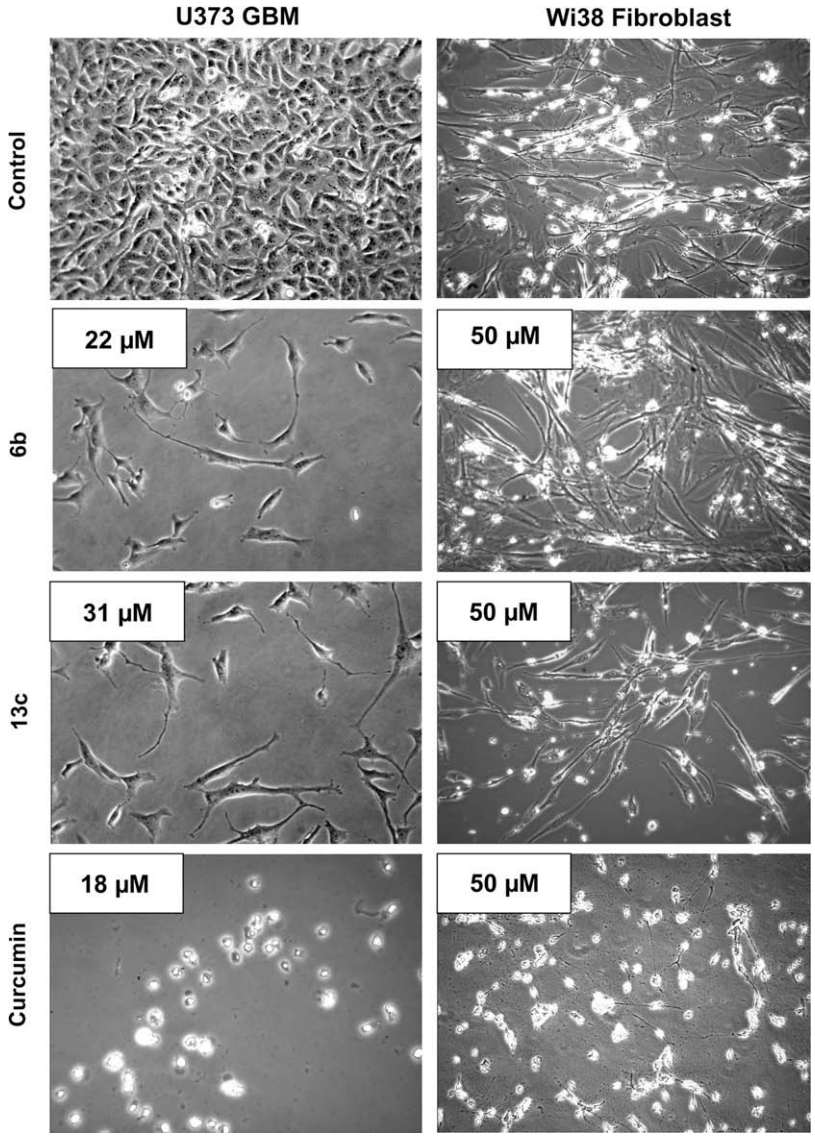

Figure 4. Illustration of modest levels of bioselectivity observed for compounds **6b** and **13c**, but the absence of bioselectivity for curcumin (**23**). The compounds were assayed at their respective IC_{50} in vitro growth inhibitory concentrations, that is, 22 μM for **6b** (Table 1), 31 μM for **13c** (Table 1), and 18 μM for **23** (Table 1), in the human U373 glioblastoma cell line and 50 μM for the three compounds in the human Wi38 fibroblast cell line. The cell lines were challenged with the compounds for 72 h and the morphological illustrations are shown in the figure. Bioselectivity is defined as the mean IC_{50} (normal cells lines)/mean IC_{50} (tumor cell lines) ratio. The bioselectivity indices are provided in Table 2.

of any specificity of inhibitory activity of a given compound for a given Aurora kinase (data not shown).

In conclusion, the current study reveals that very simple divanillic or trivanillic polyphenols display promising anticancer cytostatic activity through multi-kinase inhibition (including Aurora A, B, and C, and WEE1) and exhibit modest levels of bioselectivity. Compounds **6b** (a divanillate) and **13c** (a trivanillate) could serve as hits for optimization of the cytostatic activity through the improvement of the efficacy in inhibiting kinases over expressed in cancer as compared to normal cells, and therefore the bioselectivity of this type of polyphenols.

3. Experimental

3.1. General experimental procedures

3.1.1. Chemistry

3.1.1.1. General methods. Before their use, the solvents were distilled and dried by standard methods, that is, THF and ether from Na/benzophenone, CH_2Cl_2 and toluene from $CaCl_2$. The ^1H NMR and ^{13}C NMR spectra were recorded on a BRUKER AVANCE 300 instrument (Brucker, Wissembourg, France) in $CDCl_3$ or DMSO-d_6 or a mixture for solubility reasons. For compounds **22a**, and **22b**, 1D spectra and NOE difference experiments were recorded on a VARIAN VNMR SYSTEM 600. The chemical shifts δ are in ppm and the coupling constants J are in Hz. Analytical thin-layer chromatography was carried out on Macherey–Nagel SILG/UV_{254} precoated silica gel plates (0.25 mm) and visualization was performed by UV and/or by development using a 5% solution of phosphomolybdic acid in ethanol (heating to 110 °C for 5–20 min). Flash column chromatography was carried out using (40–63 μm) silica gel at moderate pressure. HPLC analyses were performed on an Agilent 1100 series HPLC system (Agilent, Diegem, Belgium). The chromatographic system was an ultrasphere 5μ × 4.6 mm × 250 mm C18 (Beckman Coulter (Analis, Namur, Belgium)) using the same mobile phase for all compounds (except **13b** and **13c**): MeOH–water 50:50 to 100:0 for 10 min, then 100:0 for 15 min. For

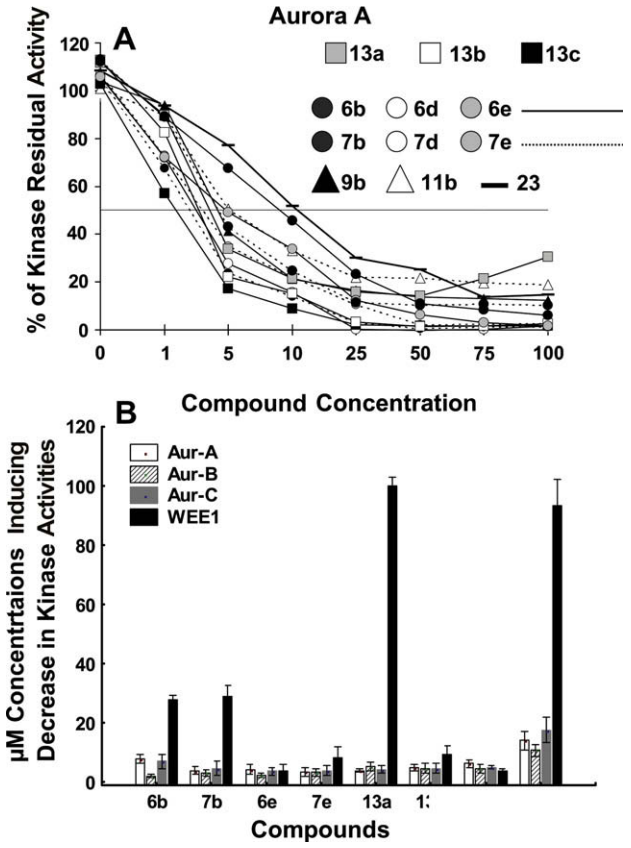

Figure 5. (A): Dose–response curves of Aurora A residual activity with compounds **6b**, **7b**, **6d**, **7d**, **6e**, **7e**, **9b**, **11b**, **13a**, **13b**, **13c**, and **23** (curcumin). (B) Concentrations (μM) inducing 50% decrease in Aurora A, B, C, and WEE1 kinase activities. The data are presented as means ± SEM values calculated in triplicates.

13b and **13c**, the mobile phase was 70% H_2O/30% MeCN + 0.1% TFA without gradient. The detection system was an agilent Diode Array Detector G1315B (monitoring wavelength given for each compound) (Agilent, Diegem, Belgium). The purity given is the purity measured by this HPLC method but we are aware of the fact that it does not take into account the co-crystallized solvents detected by NMR and elemental analysis. When there are some, the elemental analysis gives the compound-to-solvent molar ratio. The elemental analyses were recorded on a thermo Flash EA1112 series elemental analyzer (Thermo Electron Corporation, Rodano, Italy) and were within ±0.4% of the theoretical values. Mass spectra (ESI, positive mode) were recorded using a Q-TOF 6520 (Agilent, Palo Alto, CA, USA). The error between the measured exact mass and the calculated exact mass is expressed in ppm. Below 3 ppm, the compounds were considered to have the predicted formula. The infra-red spectra were recorded as KBr pellets on a Perkin Elmer 1750 FT-spectrophotometer (Perkin–Elmer, Waltham, MA, USA) and the wavelength are expressed in cm^{-1}.

3.1.1.2. General procedure for one step selective alkylation of benzoic acid derivatives bearing unprotected phenol function(s) with dibromo- or dichloroalkanes. An alkylating agent (100–300 mg, 1 equiv), a required substituted benzoic acid (1.1 equiv) and $NaHCO_3$ (1.1 equiv per halide) are added to DMF (7 mL for 100 mg of starting material) and the reaction mixture is heated at 105–110 °C overnight. A partition between water and AcOEt is then performed. The aqueous phase is extracted three times with AcOEt and organic phases are dried over Na_2SO_4, filtered and concentrated in vacuo. The crude product obtained is then purified by silica gel chromatography using an eluent specified for the R_f of each product.

3.1.1.3. General procedure for the three-step synthesis using benzyl ether as phenol protecting group. *Selective protection of the phenol function of vanillic acid*: To a stirred solution of a required substituted benzoic acid (1 equiv) in THF (15 mL), a solution of NaOH (2.5 equiv) in water (37 mL) is added. This mixture is cooled to 0 °C and benzyl chloride (4.1 mL, 34.8 mmol) is added. The reaction mixture is allowed to warm to rt and is then heated at 70 °C for 18 h. The temperature of the reaction is then raised to 90 °C for 4 h. After cooling to rt, the organic solvent is evaporated and the residual aqueous phase is acidified with 2 M HCl. The precipitate is filtered and washed with cyclohexane to afford a white solid. *Selective protection of dihydroxybenzoic and gallic acids is performed according to Baggaley et al.*[52] *esterification*: A required diol (100–200 mg), DMAP (2.1 equiv) and the phenol-protected benzylic acid derivative (2.5 equiv) are dissolved in toluene (10 mL per 100 mg diol). Then, DCC (2.3 equiv) are added. The reaction mixture is stirred at rt for 3–4 days. The solvent is evaporated to dryness and the crude product is directly purified by silica gel chromatography using an eluent given for the R_f of each product. *Deprotection*: The benzylated compound (200–500 mg, 1 equiv) is added to MeOH (20 mL for 100 mg of starting product) and the solution is cooled by a water-ice bath before the addition of the 10% Pd/C (same weight as that of the benzylated compound). This mixture is then placed under hydrogen atmosphere and stirred at rt overnight. The reaction mixture is filtered through silica gel and then a flash chromatography is performed if necessary.

3.1.1.4. Three-step synthesis involving alkylation instead of esterification. The protocols for protection and deprotection are the same as in Procedure 2. The alkylation step is described in Procedure 1.

3.1.2. Pharmacology

3.1.2.1. Determination of in vitro anticancer activity. The histological types and the origin of the 10 cancer cell lines and the two normal fibroblast cell lines are detailed in the legends to Tables 1 and 2, respectively. The 10 cancer cell lines under study were cultured in RPMI (Invitrogen, Merelbeke, Belgium) media supplemented with 10% heat inactivated fetal calf serum, 4 mM gluta mine, 100 μg/mL gentamicin, and penicillin–streptomycin (200 U/mL and 200 μg/mL) (Invitrogen). Wi38 and NHDF fibroblasts were cultured in MEM medium supplemented with 10% heat inactivated fetal bovine serum and 100 μM non-essential amino acids.

The overall growth level of human and mouse cancer cell lines, and human normal cell lines, was determined using the colorimetric MTT (3-[4,5-dimethylthiazol-2yl-diphenyl tetrazolium bromide, Sigma, Belgium) assay.[20,21] Briefly, the cell lines were incubated for 24 h in 96-microwell plates (at a concentration of 10,000–40,000 cells/mL culture medium depending on the cell type) to ensure adequate plating prior to cell growth determination. The assessment of cell population growth by means of the MTT colorimetric assay is based on the capability of living cells to reduce the yellow product MTT to a blue product, formazan, by a reduction reaction occurring in the mitochondria. The number of living cells after 72 h of culture in the presence (or absence: control) of the various compounds is directly proportional to the intensity of the blue, which is quantitatively measured by spectrophotometry—in our case using a Biorad Model 680XR (Biorad, Nazareth, Belgium) at a 570 nm wavelength (with a reference of 630 nm). Each experiment was carried out in sextuplicate.

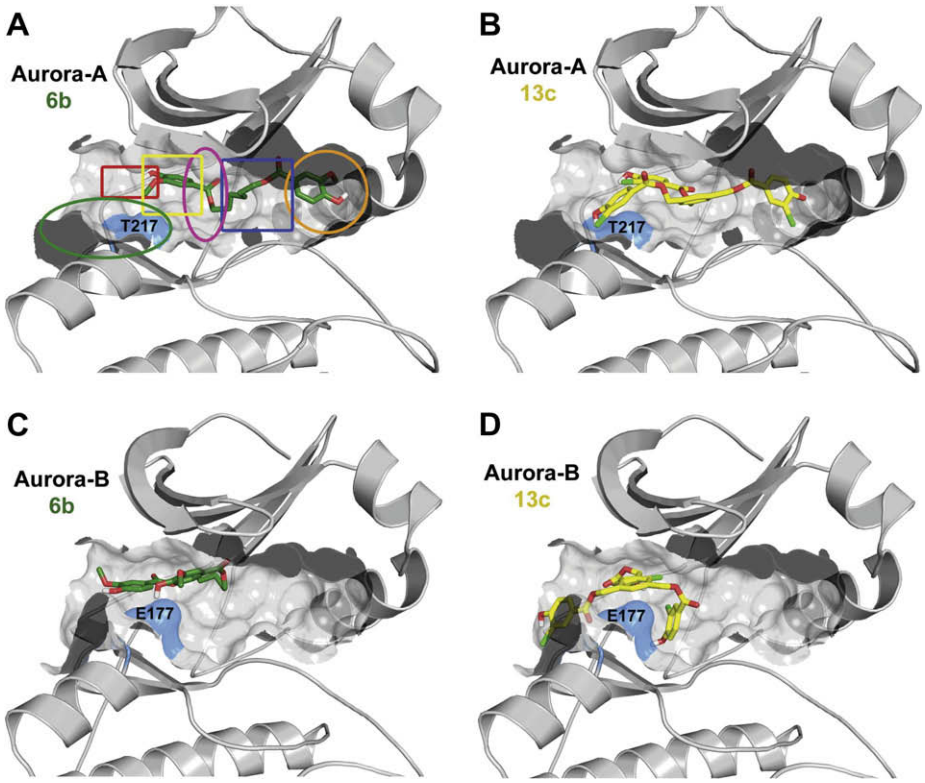

Figure 6. Best solutions of the docking experiments performed with compound **6b** (green) and **13c** (yellow) in the active site of Aurora A (panels A and B) and B (panels C and D). The overall structures of the proteins are shown as cartoons and the area surrounding the compounds as a transparent surface. The blue area highlights the residue substitution between Aurora A (T217) and B (E177) close to the nucleotide-binding pocket. The different regions of the Aurora active site are highlighted in panel A: solvent accessible (green), hinge (red), purine binding (yellow), sugar binding (magenta), phosphate binding (blue), and hydrophobic (orange) regions.

3.1.2.2. Quality controls for the determination of in vitro anticancer activity. The direct visualization of compound-induced effects on cell proliferation and cell migration was carried out by means of computer-assisted phase-contrast microscopy, that is, quantitative videomicroscopy as detailed elsewhere.[53,54]

3.1.2.3. Kinase activity determination. The profiling of compounds **6b** (carried out at 20 μM) and **13c** (carried out at 2 μM) has been performed at ProQinase GmbH (Freiburg, Germany) on 256 human protein kinases which are listed in Table 3 (in the Supplementary data) along with their substrates. The materials and methods used by ProQinase to perform these assays are fully detailed in the Supplementary data. Compounds **6b** and **13c** were tested twofold in singlicate in each kinase assay. This assay was carried out in order to identify which kinase had residual activity decreased by at least 50% with 20 μM **6b** and by at least 75% with 2 μM **13c**. Then, compounds **1b**, **2b**, **3b**, **4g**, **6a**, **6b**, **6c**, **6d**, **6e**, **7a**, **7b**, **7c**, **7d**, **7e**, **9b**, **11b**, **12b**, **13a**, **13b**, **13c**, **17a**, **17b**, and **17c** were tested in triplicate at each of the eight concentrations, that is, 0 (control), 1, 5, 10, 25, 50, 75, and 100 μM in the Aurora A, Aurora B, Aurora C, and WEE1 kinase assays. This second set of experiments was carried out to determine the IC_{50} concentration of the compound leading to 50% of kinase residual activity.

3.1.2.4. Molecular docking. The crystallographic structures of the human Aurora A and the *Xenopus laevis* Aurora B with the respective PDB code 1OL5[55] and 2VRX[56] were selected to perform the docking experiments. The two structures were chosen for their open active sites whose superimposition exhibits the lowest root mean square deviation calculated for residues within 10 Å around the active site. The structures were prepared for docking study as follows: for both proteins, water molecules were removed from and hydrogen atoms were added to the PDB files; Gasteiger charges were merged to the receptor. For compounds **6b** and **13c**, Gasteiger charges were assigned and non-polar hydrogen atoms were merged.

The docking energy grids were calculated with the program AutoGrid. The grid dimensions were $78 \times 84 \times 70$ points along the *x*-, *y*-, and *z*-axes, with points separated by 0.375 Å. The grids were chosen to include the entire ATP binding site as well as a region potentially involved in ligand binding, and cover the positions of all the cofactors and inhibitors in complex with Aurora A or B available in the Protein Data Bank. Ligand docking was performed using the Lamarckian genetic algorithm implemented in AUTODOCK 4.1.[57] The energy evaluations, number of individuals in the population and number of runs were, respectively, set to 25×10^6, 250, and 50. Other parameters were set to default values. The figure presenting the solution with the lowest energy was generated using Pymol.[58]

Acknowledgments

The authors thank the Fonds National de la Recherche Scientifique (FNRS, Belgium), the Fonds Yvonne Boël (Belgium) and the National Institutes of Health (USA, CA135579) for financial support of this work. Robert Kiss is a director of research, Florence Lefranc a MD, Postdoctoral Fellow, and Frederic Kerff a PhD, Postdoctoral Fellow with the FNRS. We greatly thank Amandine Djeffal for her excellent technical assistance.

Supplementary data

Supplementary data (the characterization data for all compounds synthesized and biologically evaluated in this study (HPLC, ^{1}H NMR, ^{13}C NMR, mass spectra, etc.), as well as detailed biological

and biochemical protocols) associated with this article can be found, in the online version, at doi:10.1016/j.bmc.2010.04.047.

References and notes

1. Simpson, C. D.; Anyiwe, K.; Schimmer, A. D. *Cancer Lett.* **2008**, *272*, 177.
2. Savage, P.; Stebbing, J.; Bower, M.; Crook, T. *Nat. Clin. Pract. Oncol.* **2009**, *6*, 43.
3. Wilson, T. R.; Johnston, P. G.; Longley, D. B. *Curr. Cancer Drug Targets* **2009**, *9*, 307.
4. Bozec, A.; Peyrade, F.; Fischel, J. L.; Milano, G. *Expert Opin. Emerg. Drugs* **2009**, *14*, 299.
5. Capdevilla, J.; Ramos, F. J.; Macarulla, T.; Elez, E.; Ruiz-Echarri, M.; Perez-Garcia, J.; Tabernero, J. *Curr. Opin. Oncol.* **2009**, *21*, 374.
6. Lefranc, F.; Brotchi, J.; Kiss, R. *J. Clin. Oncol.* **2005**, *23*, 2411.
7. Soengas, M. S.; Lowe, S. W. *Oncogene* **2003**, *22*, 3138.
8. Li, B.; Li, Y. Y.; Tsao, S. W.; Cheung, A. L. *Mol. Cancer Ther.* **2009**, *8*, 2635.
9. Mathieu, A.; Remmelink, M.; D'Haene, N.; Penant, S.; Gaussin, J. F.; Van Ginckel, R.; Darro, F.; Kiss, R.; Salmon, I. *Cancer* **2004**, *101*, 1908.
10. Ramsay, A. K.; Leung, H. Y. *Clin. Sci. (Lond.)* **2009**, *117*, 209.
11. Smalley, K. S. *J. Invest. Dermatol.* **2010**, *130*, 28.
12. Khan, N.; Afaq, F.; Saleem, M.; Ahmad, N.; Mukhtar, H. *Cancer Res.* **2006**, *66*, 2500.
13. Banerjee, S.; Li, Y.; Wang, Z.; Sarkar, F. H. *Cancer Lett.* **2008**, *269*, 226.
14. Ravindran, J.; Prasad, S.; Aggarwal, B. B. *AAPS J.* **2009**, *11*, 495.
15. Lamoral-Theys, D.; Pottier, L.; Dufrasne, F.; Nève, J.; Dubois, J.; Kornienko, A.; Kiss, R.; Ingrassia, L. *Curr. Med. Chem.* **2010**, *17*, 812.
16. Korkina, L. G.; De Luca, C.; Kostyuk, V. A.; Pastore, S. *Curr. Med. Chem.* **2009**, *16*, 3943.
17. Cuccioloni, M.; Mozzicafreddo, M.; Bonfili, L.; Cecarini, V.; Eleuteri, A. M.; Angeletti, M. *Chem. Biol. Drug. Des.* **2009**, *74*, 1.
18. Yang, C. S.; Wang, X.; Lu, G.; Picinich, S. C. *Nat. Rev. Cancer* **2009**, *9*, 429.
19. Reuter, S.; Eifes, S.; Dicato, M.; Aggarwal, B. B.; Diederich, M. *Biochem. Pharmacol.* **2008**, *76*, 1340.
20. Ingrassia, L.; Lefranc, F.; Dewelle, J.; Pottier, L.; Mathieu, V.; Spiegl-Kreinecker, S.; Sauvage, S.; El Yazidi, M.; Dehoux, M.; Berger, W.; Van Quaquebeke, E.; Kiss, R. *J. Med. Chem.* **2009**, *52*, 1100.
21. Lamoral-Theys, D.; Andolfi, A.; Van Goietsenoven, G.; Le Calvé, B.; Wauthoz, N.; Mégalizzi, V.; Gras, T.; Bruyère, C.; Dubois, J.; Mathieu, V.; Kornienko, A.; Kiss, R.; Evidente, A. *J. Med. Chem.* **2009**, *52*, 6244.
22. Lirdprapamongkol, K.; Kramb, J. P.; Suthiphongchai, T.; Surarit, R.; Srisomsap, C.; Dannhardt, G.; Svasti, J. *J. Agric. Food Chem.* **2009**, *57*, 3055.
23. Lirdprapamongkol, K.; Sakurai, H.; Kawasaki, N.; Choo, M. K.; Saitoh, Y.; Aozuka, Y.; Singhirunnusorn, P.; Ruchirawat, S.; Svasti, J.; Saiki, I. *Eur. J. Pharm. Sci.* **2005**, *25*, 57.
24. Bruggisser, R.; von Daeniken, K.; Jundt, G.; Schaffer, W.; Tullberg-Reinert, H. *Planta Med.* **2002**, *68*, 445.
25. Branle, F.; Lefranc, F.; Camby, I.; Jeuken, J.; Geurts-Moespot, A.; Sprenger, S.; Sweep, F.; Kiss, R.; Salmon, I. *Cancer* **2002**, *95*, 641.
26. Mijatovic, T.; Mathieu, V.; Gaussin, J. F.; De Nève, N.; Ribaucour, F.; Van Quaquebeke, E.; Dumont, P.; Darro, F.; Kiss, R. *Neoplasia* **2006**, *5*, 402.
27. Bruyere, C.; Mijatovic, T.; De Neve, N.; Gaussin, J. F.; Gras, T.; Nindfa, P.; Dehoux, M.; Saussez, S.; Kiss, R. In *Proceedings of the 100th Annual Meeting of the American Association for Cancer Research*; 2009 Apr 18–22; AACR: Denver, CO. Philadelphia (PA), 2009; Abstract no. 4135.
28. Dumont, P.; Ingrassia, L.; Rouzeau, S.; Ribaucour, F.; Thomas, S.; Roland, I.; Darro, F.; Lefranc, F.; Kiss, R. *Neoplasia* **2007**, *9*, 766.
29. Mathieu, V.; Pirker, C.; Martin de Lasalle, E.; Vernier, M.; Mijatovic, T.; De Neve, N.; Gaussin, J. F.; Dehoux, M.; Lefranc, F.; Berger, W.; Kiss, R. *J. Cell. Mol. Med.* **2009**, *13*, 3960.
30. Patani, G. A.; LaVoie, E. J. *Chem. Rev.* **1996**, *96*, 3147.
31. Boss, D. S.; Beijnen, J. H.; Schellens, J. H. M. *Oncologist* **2009**, *14*, 780.
32. Garuti, L.; Roberti, M.; Bottegoni, G. *Curr. Med. Chem.* **2009**, *16*, 1949.
33. Jeon, S.; Choi, J. Y.; Lee, K. M.; Park, S. K.; Yoo, K. Y.; Noh, D. Y.; Ahn, S. H.; Kang, D. *Breast Cancer Res. Treat.* **2009**, in press.
34. Ali, S.; Heathcote, D. A.; Kroll, S. H.; Jogalekar, A. S.; Scheiper, B.; Patel, H.; Brackow, J.; Siwicka, A.; Fuchter, M. J.; Periyasamy, M.; Tolhurst, R. S.; Kanneganti, S. K.; Snyder, J. P.; Liotta, D. C.; Aboagye, E. O.; Barrett, A. G.; Coombes, R. C. *Cancer Res.* **2009**, *69*, 6208.
35. Li, H.; Ren, Z.; Kang, X.; Zhang, L.; Li, X.; Wang, Y.; Xue, T.; Shen, Y.; Liu, Y. *BMC Cancer* **2009**, *9*, 366.
36. Zoubeidi, A.; Rocha, J.; Zouanat, F. Z.; Hamel, L.; Scarlata, E.; Aprikian, A. G.; Chevalier, S. *Mol. Cancer Res.* **2009**, *7*, 142.
37. Sun, Y. *Mol. Carcinog.* **2006**, *45*, 409.
38. Li, J.; Tan, M.; Li, L.; Pamarthy, D.; Lawrence, T. S.; Sun, Y. *Neoplasia* **2005**, *7*, 312.
39. Kellogg, D. R. *J. Cell Sci.* **2003**, *116*, 4883.
40. Jun, P.; Hong, C.; Lal, A.; Wong, J. M.; McDermott, M. W.; Bollen, A. W.; Plas, C.; Held, W. A.; Smiraglia, D. J.; Costello, J. F. *Neuro. Oncol.* **2009**, *11*, 414.
41. Moniz, S.; Verissimo, F.; Matos, P.; Brazao, R.; Silva, E.; Kotelevets, L.; Chastre, E.; Gespach, C.; Jordan, P. *Oncogene* **2007**, *26*, 6071.
42. Druker, B. J. *Mol. Cancer Ther.* **2003**, *2*, 225.
43. Hampton, T. *JAMA* **2004**, *292*, 419.
44. Daub, H.; Specht, K.; Ullrich, A. *Nat. Rev. Cancer* **2004**, *3*, 1001.
45. Frantz, S. *Nature* **2005**, *437*, 942.
46. Csermely, P.; Agoston, V.; Pongor, S. *Trends Pharmacol. Sci.* **2005**, *26*, 178.
47. Zaidi, S. H.; Huddart, R. A.; Harrington, K. J. *Curr. Drug Discov. Technol.* **2009**, *6*, 103.
48. Hwang, M.; Moretti, L.; Lu, B. *Curr. Med. Chem.* **2009**, *16*, 3081.
49. Sarkar, F. H.; Li, Y. *Cancer Treat. Rev.* **2009**, *35*, 597.
50. Dubinina, G. G.; Chupryna, O. O.; Platonov, M. O.; Borisko, P. O.; Ostrovska, G. V.; Tolmachov, A. O.; Shtil, A. A. *Anticancer Agents Med. Chem.* **2007**, *7*, 171.
51. Aliagas-Martin, I.; Burdick, D.; Corson, L.; Dotson, J.; Drummond, J.; Fields, C.; Huang, O. W.; Hunsaker, T.; Kleinheinz, T.; Krueger, E.; Liang, J.; Moffat, J.; Phillips, G.; Pulk, R.; Rawson, T. E.; Ultsch, M.; Walker, L.; Wiesmann, C.; Zhang, B.; Zhu, B. Y.; Cochran, A. G. *J. Med. Chem.* **2009**, *52*, 3300.
52. Baggaley, K. H.; Fears, R.; Hindley, R. M.; Morgan, B.; Murrel, E.; Thorne, D. E. *J. Med. Chem.* **1977**, *20*, 1388.
53. De Hauwer, C.; Camby, I.; Darro, F.; Migeotte, I.; Decaestecker, C.; Verbeek, C.; Danguy, A.; Pasteels, J. L.; Brotchi, J.; Salmon, I.; Van Ham, P.; Kiss, R. *J. Neurobiol.* **1998**, *37*, 373.
54. Delbrouck, C.; Doyen, I.; Belot, N.; Decaestecker, C.; Ghanooni, R.; de Lavareille, A.; Kaltner, G.; Choufani, G.; Danguy, A.; Vandenhoven, G.; Gabius, H. J.; Hassid, S.; Kiss, R. *Lab. Invest.* **2002**, *82*, 147.
55. Bayliss, R.; Sardon, T.; Vernos, I.; Conti, E. *Mol. Cell* **2003**, *12*, 851.
56. Girdler, F.; Sessa, F.; Patercoli, S.; Villa, F.; Musacchio, A.; Taylor, S. S. *Chem. Biol.* **2008**, *15*, 552.
57. Huey, R.; Morris, G. M.; Olson, A. J.; Goodsell, D. S. *Comput. Chem.* **2007**, *28*, 1145.
58. DeLano, W. L. DeLano Scientific, San Carlos, CA, USA. The PyMOL Molecular Graphics System, 2002.